Ultrasound in Med. & Biol., Vol. ■■, No. ■■, pp. ■■–■■, 2017

0301-5629/$ - see front matter

https://doi.org/10.1016/j.ultrasmedbio.2017.10.010

● *Original Contribution*

AN ULTRASOUND SURFACE WAVE TECHNIQUE FOR ASSESSING SKIN AND LUNG DISEASES

Xiaoming Zhang,[*,†] Boran Zhou,[*] Sanjay Kalra,[‡] Brian Bartholmai,[*] James Greenleaf,[†] and Thomas Osborn[§]

[*] Department of Radiology, Mayo Clinic, Rochester, Minnesota, USA; [†] Department of Physiology and Biomedical Engineering, Mayo Clinic, Rochester, Minnesota, USA; [‡] Department of Pulmonary and Critical Care Medicine, Mayo Clinic, Rochester, Minnesota, USA; and [§] Department of Rheumatology, Mayo Clinic, Rochester, Minnesota, USA

(*Received* 11 *August* 2017; *revised* 28 *September* 2017; *in final form* 19 *October* 2017)

Abstract—Systemic sclerosis (SSc) is a multi-organ connective tissue disease characterized by immune dysregulation and organ fibrosis. Severe organ involvement, especially of the skin and lung, is the cause of morbidity and mortality in SSc. Interstitial lung disease (ILD) includes multiple lung disorders in which the lung tissue is fibrotic and stiffened. The purpose of this study was to translate ultrasound surface wave elastography (USWE) for assessing patients with SSc and/or ILD *via* measuring surface wave speeds of both skin and superficial lung tissue. Forty-one patients with both SSc and ILD and 30 healthy patients were enrolled in this study. An external harmonic vibration was used to generate the wave propagation on the skin or lung. Three excitation frequencies of 100, 150 and 200 Hz were used. An ultrasound probe was used to measure the wave propagation in the tissue non-invasively. Surface wave speeds were measured on the forearm and upper arm of both left and right arm, as well as the upper and lower lungs, through six intercostal spaces of patients and healthy patients. Viscoelasticity of the skin was calculated by the wave speed dispersion with frequency using the Voigt model. The magnitudes of surface wave speed and viscoelasticity of patients' skin were significantly higher than those of healthy patients ($p < 0.0001$) for each location and each frequency. The surface wave speeds of patients' lung were significantly higher than those of healthy patients ($p < 0.0001$) for each location and each frequency. USWE is a non-invasive and non-ionizing technique for measuring both skin and lung surface wave speed and may be useful for quantitative assessment of SSc and/or ILD. (E-mail: zhang.xiaoming@mayo.edu) **© 2017 World Federation for Ultrasound in Medicine & Biology. All rights reserved.**

Key Words: **Ultrasound surface wave elastography, Skin, Lung, Scleroderma, Interstitial lung disease.**

INTRODUCTION

Systemic sclerosis (SSc), also termed scleroderma, is a multi-organ connective tissue disease characterized by immune dysregulation and organ fibrosis (Steen and Medsger 2000). Thickening of the skin, often the earliest affected organ, is considered an early marker of disease activity in SSc (Steen and Medsger 2000). Severe organ involvement, especially of the skin and lung, is the cause of morbidity and mortality in SSc. The degree of skin involvement is a predictor of mortality (Clements et al. 1990). Improvement in skin stiffness is associated with improved survival in many clinical trials (Steen and Medsger 2001). Patients who do not develop severe organ involvement in the first few years are less likely to develop life-threatening involvement later throughout the course of the disease. The modified Rodnan skin score (MRSS) is the standard skin assessment tool in the majority of clinical studies of SSc (Abignano et al. 2011). Patients with an improved MRSS after 2 y of treatment have improved survival (Steen and Medsger 2001). The MRSS is commonly used as an outcome measure in clinical trials (Clements et al. 2000). However, the MRSS is a palpation method, which is subjective, and thus, its accuracy is user dependent (Clements et al. 1995). Moreover, it is difficult to measure the change in skin stiffness over time using palpation (Postlethwaite et al. 2008).

Skin stiffness can be measured using durometry (Kissin et al. 2006; Merkel et al. 2008), indentation (Boyer et al. 2009; Pailler-Mattei et al. 2008; Serup and Jemec 1995) and cutometers (Hendriks et al. 2006; Smalls et al. 2006). In durometry, a piston-spring-dial handheld

Address correspondence to: Xiaoming Zhang, Department of Radiology, Mayo Clinic, 200 1st Street SW, Rochester, MN 55905, USA. E-mail: zhang.xiaoming@mayo.edu

apparatus is used to measure skin hardness. However, durometry readings are affected by the experience of users. Indentation is the technique of measuring elasticity by indenting the material. The cutometer measures skin displacement in response to a suction force. Because its measurements depend on the interactions between a probe and the skin, deeper skin layers must be measured with larger probes (Hendriks et al. 2006). Notably, these techniques cannot evaluate subcutaneous tissue.

Patients with interstitial lung disease (ILD) have fibrotic and stiff lungs causing symptoms, especially dyspnea, and may eventually lead to respiratory failure (Coultas et al. 1994). Many ILDs typically are distributed in the peripheral, subpleural regions of the lung (Desai et al. 2004; Wells et al. 1993). High-resolution computed tomography (HRCT) is the clinical standard for diagnosing lung fibrosis (Mathieson et al. 1989; Verschakelen 2010), but it substantially increases radiation exposure for patients. Various scanning techniques have been proposed to reduce the dose (Mayo 2009). Intercostal ultrasound can be used to avoid ionizing radiation during follow-up visits (Delle Sedie et al. 2012). However, it is not able to quantify lung stiffness.

Currently, no clinical approach is available to noninvasively quantify and evaluate the progression and development of SSc and ILD. Therefore, there is a pressing need to develop an accurate and reproducible clinical technique for quantification and tracking of the disease and to develop effective treatment for sclerosis and fibrotic disorders (Lott and Girardi 2011). The research described here was aimed at translating an ultrasound surface wave elastography (USWE) technique into clinical use for quantitative assessment of patients with SSc and ILD.

METHOD

Raleigh surface wave equation

Surface wave propagation can be analyzed as wave propagation in a semi-infinite linear elastic medium under a local harmonic excitation on the surface. The equation for wave propagation in an isotropic and elastic medium is (Miller and Pursey 1954)

$$(\lambda+2\mu)\nabla\nabla.\vec{u}-\mu\nabla\times\nabla\times\vec{u}=\rho\frac{\partial^2\vec{u}}{\partial t^2}, \qquad (1)$$

where $\vec{u}$ is the displacement vector, ρ is the mass density and λ and μ are the Lamé coefficients of the medium. For linear viscoelastic material, $\lambda = \lambda_1 + \partial\lambda_2/\partial t$ and $\mu = \mu_1 + \partial\mu_2/\partial t$, where λ_1, λ_2, μ_1 and μ_2 are the coefficients of volume compressibility, volume viscosity, shear elasticity and shear viscosity, respectively.

Surface wave propagation can be solved in the cylindrical polar coordinate system as illustrated in Figure 1. Consider a harmonic force excitation with uniform stress on the surface of the medium in the circular region of $r \le a$.

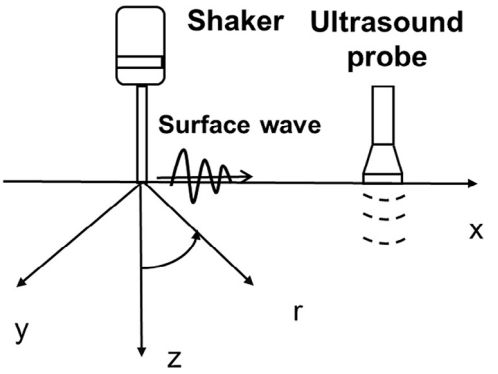

Fig. 1. Schematic of surface wave generation and detection on the skin. The skin surface is on the plane of x- and y-coordinates. The surface wave on the skin is generated by a handheld electromechanical shaker through a ball-tip applicator on the skin. The vibration excitation is typically a 0.1-s harmonic signal at a frequency between 100 and 200 Hz. The resulting surface wave propagation on the skin is measured using an ultrasound probe. A standoff gel pad is used between the ultrasound probe and skin to improve imaging of the skin. The surface wave speed depends on the local elastic properties of the skin and is independent of the location of wave generation.

The displacement fields are derived in the r and z directions at any location in and on the surface of the medium as (Miller and Pursey 1954)

$$\begin{aligned} u_z &= \frac{a}{\mu}\int_0^\infty \frac{\sqrt{(\xi^2-1)}J_1(\xi k_1 a)}{F_0(\xi)}\Big\{2\xi^2 e^{-k_1 z\sqrt{(\xi^2-\eta^2)}} \\ &\quad + (\eta^2-2\xi^2)e^{-k_1 z\sqrt{(\xi^2-1)}}\Big\}J_0(\xi k_1 r)\,d\xi \\ u_r &= \frac{a}{\mu}\int_0^\infty \frac{\xi J_1(\xi k_1 a)}{F_0(\xi)}\Big\{2\sqrt{(\xi^2-1)}\sqrt{(\xi^2-\eta^2)}e^{-k_1 z\sqrt{(\xi^2-\eta^2)}} \\ &\quad + (\eta^2-2\xi^2)e^{-k_1 z\sqrt{(\xi^2-1)}}\Big\}J_1(\xi k_1 r)\,d\xi, \end{aligned} \qquad (2)$$

where a is the radius of the distributed stress, and ξ is the integration parameter in the wavenumber domain, which has been normalized with respect to k_1. The divisor function of the integration functions is $F_0(\xi) = (2\xi^2-\eta^2)^2 - 4\xi^2\sqrt{(\xi^2-1)}\sqrt{(\xi^2-\eta^2)}$, where $\eta = k_2/k_1 = \sqrt{\{2(1-\sigma)/(1-2\sigma)\}}$ and $k_1 = \omega\sqrt{\rho/(\lambda+2\mu)}$, $k_2 = \omega\sqrt{\rho/\mu}$, where ω is the angular frequency, ρ is the density, σ is Poisson's ratio for the medium, k_1 and k_2 denote the wavenumbers for compression and shear wave propagation, respectively, and J_0 and J_1 refer to Bessel functions of the first kind.

The wave displacement fields can be solved with eqn (2). However, using the displacements to estimate the elastic properties of the medium depends on the excitation and boundary conditions. Because the wave propagation is dependent on local medium properties, we used the surface

wave speed measurement to estimate the viscoelastic properties of the medium. The surface wave speed can be solved by (Zhang and Greenleaf 2007)

$$\left(2\xi^2-\eta^2\right)^2-4\xi^2\sqrt{\left(\xi^2-1\right)}\sqrt{\left(\xi^2-\eta^2\right)}=0 \tag{3}$$

Equation (3) is a bi-fourth equation of ξ; however, only the solution for which ξ is real, $\xi > \eta$ and $\xi > 1$, is the right solution for the surface wave.

Equation (3) has been studied by Nkemzi (1997) and us (Zhang and Greenleaf 2007). Several approximations have been proposed to solve the surface wave speed (Royer and Clorennec 2007; Twal et al. 2014; Viktorov 1976; Vinh and Malischewsky 2007). The relationship between shear wave speed c_2 and the surface wave speed c_s is approximated by (Royer and Clorennec 2007)

$$\frac{c_2}{c_s}=\sqrt{\frac{0.58+K}{0.44+K}} \tag{4}$$

where $K=\sigma/(1-\sigma)$, and σ is Poisson's ratio of the medium. The speed of shear waves is slightly greater than that of surface waves for all materials from metals to soft tissues. Because soft tissues are generally incompressible and their Poisson ratios lie in the narrow region between 0.45 and 0.50, $c_2=1.05c_s$ can be obtained from eqn (4). The surface wave speed can be related to the elastic modulus of tissue as (Zhang and Greenleaf 2007)

$$c_s=\frac{1}{1.05}\sqrt{\frac{\mu}{\rho}} \tag{5}$$

where μ is the shear elasticity in Pascal and ρ is the mass density of the tissue (in kg/m^3).

Voigt's viscoelastic model: wave dispersion curve

For soft tissue under low-frequency harmonic excitation, Voigt's model, which consists of a spring of elasticity μ_1 and a damper of viscosity μ_2 connected in parallel, has been proven to be effective in modeling linear viscoelastic materials (Catheline et al. 2004; Chen et al. 2009; Prim et al. 2016; Zhou et al. 2017). The wave dispersion curve of wave speed c_s with respect to the excitation frequency ω can be formulated as

$$c_s=\frac{1}{1.05}\sqrt{\frac{2\left(\mu_1^2+\omega^2\mu_2^2\right)}{\rho\left(\mu_1+\sqrt{\mu_1^2+\omega^2\mu_2^2}\right)}} \tag{6}$$

Cross-spectrum: phase gradient method

In USWE, a 0.1-s harmonic vibration at a specific frequency is generated on the skin, and the resulting time response of the skin is measured using an ultrasound probe. If $s_1(t)$ and $s_2(t)$ represent the displacement responses at two locations on the skin, the phase change of surface wave propagation over the two locations can be calculated with the cross-spectrum method. The cross-spectrum $S(f)$ of two signals $s_1(t)$ and $s_2(t)$ is defined as (Hasegawa and Kanai 2006),

$$S(f)=S_1^*(f)\cdot S_2(f)=\left|S_1(f)\cdot S_2(f)\right|\cdot e^{-j\Delta\varphi(f)} \tag{7}$$

where $S_1(f)$ and $S_2(f)$ are the Fourier transforms of $s_1(t)$ and $s_2(t)$, respectively; * denotes the complex conjugate; and $\Delta\phi\,(f)$ is the phase change between $s_1(t)$ and $s_2(t)$ over distance at frequency f.

The phase change of the surface wave with distance is used to measure the surface wave speed,

$$c_s=2\pi f\left|\Delta r/\Delta\phi\right| \tag{8}$$

where Δr is the radial distance of two measuring locations, $\Delta\phi$ is the wave phase change over distance and f is the frequency.

The estimation of wave speed can be improved by using multiple phase change measurements over distance. The regression of the phase change $\Delta\phi$ with distance Δr can be obtained by "best fitting" a linear relationship between them,

$$\widehat{\Delta\phi}=\alpha\Delta r+\beta \tag{9}$$

where $\widehat{\Delta\phi}$ denotes the value of $\Delta\phi$ on the regression for a given distance of Δr, and α is the regression parameter.

The surface wave speed can be estimated as

$$c_{sr}=2\pi f\left|\Delta r/\widehat{\Delta\phi}\right|=2\pi f/\alpha \tag{10}$$

where C_{sr} is the estimation of wave speed from the regression analysis.

Human study protocol

Human studies were approved by the Mayo Clinic institutional review board. Each participant completed an informed consent form. Patients were enrolled in this research based on their clinical diagnoses. We enrolled 41 patients with SSc and ILD from the Mayo Clinic Departments of Rheumatology and Pulmonary and Critical Care Medicine. These patients are confirmed ILD patients with clinical assessments together with pulmonary function tests and high-resolution computed tomography (CT) scans. These patients also have a confirmed clinical diagnosis of SSc. The American College of Rheumatology (ACR) developed classification criteria for SSc (American Rheumatism Association Diagnostic and Therapeutic Criteria Committee, Subcommittee for Scleroderma Criteria 1980) . The diagnosis requires either (i) the major criterion of proximal scleroderma, as judged by palpation or

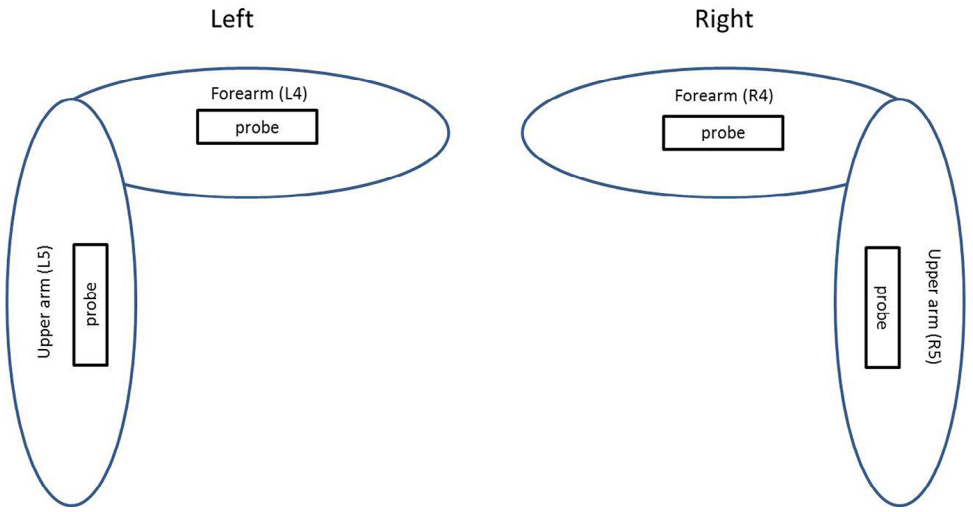

Fig. 2. Schematic of skin locations tested on human patients. *Square boxes* represent the tested positions. Probe orientation is aligned with the arm longitudinal axis. Left and right forearms and upper arms were labeled L4, L5, R4 and R5.

simple observation of the skin; or (ii) two minor criteria such as sclerodactyly, digital pitting scars or loss of substance from the finger pad and bibasilar pulmonary fibrosis. The patients enrolled in this study typically have advanced disease because fibrosis already involves the two organs of skin and lung. Further analysis of disease severity and grading using the surface wave speed measures are being carried out, and the results will be published soon. The mean age of the patients was 61.88 y (range: 37–82, 13 male and 28 female). Thirty healthy participants were enrolled as controls if they did not have any skin or lung diseases. The mean age of the healthy controls was 45.43 y (range: 22–73, 14 male and 16 female).

Participants were tested in a sitting position with their left or right forearm and upper arm placed horizontally on a pillow in a relaxed state. The skin of both left and right forearms and upper arms of patients was tested (Fig. 2). These locations were in the central part of the arms and on the dorsal sides. A 0.1-s harmonic vibration was generated by the indenter of the handheld shaker (Model FG-142, Labworks, Costa Mesa, CA, USA) on the skin of the forearm or upper arm of the participants. The excitation force from the indenter was much less than 1 N, and the participants felt only a small vibration on their skin. A Verasonics ultrasound system (Verasonics V1, Verasonics, Kirkland, WA, USA) with an L11-4 ultrasound probe with a central frequency of 6.4 MHz was used for detecting the surface wave motion of the skin. The probe had an elevation aperture of 38.4 mm and was customized to provide a 50-mm focal depth in the elevation axis. Elements were spaced at 30-μm intervals along the azimuthal axis. All images were acquired at a 50-V transmission voltage. Images of the skin and lung tissue were acquired by compounding 11 successive angles at a pulse repetition frequency (PRF) of 2 kHz. To improve the imaging quality of skin, an ultrasound gel pad standoff by Aquaflex (Parker Laboratories, Fairfield, NJ, USA) was placed between probe and skin. Surface wave speed on the skin was measured by determining the change in wave phase with distance along the skin. In Figure 3 are representative B-mode images of the skin for a patient and a healthy control. The top dark area of the image is the Aquaflex standoff gel pad. On the skin surface, eight locations were used to measure the surface wave speed of skin. The skin motion velocity was in response to the external vibration excitation induced by the handheld vibrator. Using the skin motion at the first location as a reference, the wave phase delay of the skin motions at the remaining locations, relative to the first location, was used to measure surface wave speed. The surface wave speed was measured at three excitation frequencies of 100, 150 and 200 Hz. Three measurements were performed at each location and at each frequency. Light tissue motion in the tens of micrometers was enough for sensitive ultrasound detection of the tissue motion generated. The 100-Hz excitation signal is stronger than those of higher-frequency excitations. The higher-frequency waves have smaller wavelength, but decay more rapidly over distance than the lower-frequency waves. The frequency ranges chosen in this study consider the wave motion amplitude, spatial resolution and wave attenuation.

We studied the repeatability and reproducibility of the USWE measurements on the forearm of a healthy control. Ten measurements of wave speed were performed at 100, 150 and 200 Hz. The Inter-rater reliability was evaluated with two raters' measurements. Interclass correlation coefficients (ICCs) were 0.94, 0.96 and 0.98 for wave speeds at 100, 150 and 200 Hz, respective-

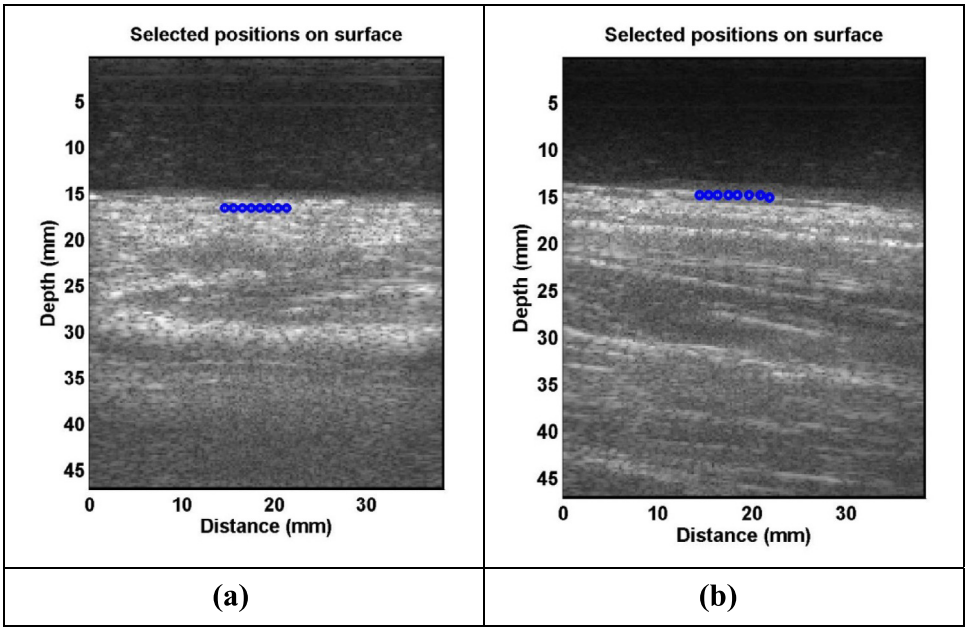

Fig. 3. Representative B-mode images of skin for a patient (a) and a healthy control (b). An ultrasound gel pad standoff was used to improve imaging of the skin. The top dark area in the image was associated with the gel pad. Eight locations on the skin surface were used to measure the surface wave speed of skin.

ly. Intra-rater reliability was evaluated with one rater's measurements 1 d and 1 wk later. At that time, the ICCs were 0.95, 0.91 and 0.95 for wave speeds at 100, 150 and 200 Hz, respectively. In these measurements, there were no statistical differences in the mean measurements between intra-rater and inter-rater data. Reproducibility and repeatability are considered "good" at ICCs ≥0.60 and ≤0.74 and "excellent" at ICCs ≥0.75 and ≤1.00 (Cicchetti 1994).

Both lungs of the participant were tested through six intercostal spaces. The upper anterior lungs were tested at the second intercostal space in the mid-clavicular line. The lower lateral lungs were tested at one intercostal space above the level of the diaphragm in the mid-axillary line. The lower posterior lungs were tested at one intercostal space above the level of the diaphragm in the mid-scapular line. The indenter of the handheld shaker is placed on the chest wall in an intercostal space. The same ultrasound system and probe were used for lung testing. The ultrasound probe is positioned about 5 mm away from the indenter in the same intercostal space to measure the resulting surface wave propagation on the lung. The lung was tested at total lung capacity in which the participant took a deep breath and held it for a few seconds. Ultrasound imaging was used to identify the lungs and select appropriate intercostal spaces to measure the upper and lower lungs. Three measurements were performed at each location and at each frequency. Typical testing lasted about 30 min.

In lung testing, a direct vibration excitation on the lung surface is not possible. Instead, the surface wave propagation on the lung is induced by a vibration excitation on the chest wall. The resulting wave propagates through the intercostal muscle and on the surface of the lung. We previously reported that surface wave propagation on the lung can be generated by a vibration excitation on the surface of muscle in an *ex vivo* muscle–lung model (Zhang et al. 2016).

Statistical analysis

An unpaired, two-tailed *t*-test of the differences between the healthy controls and the patients was conducted to compare sample means. Differences in mean values were considered significant at $p < 0.05$.

RESULTS

Figure 4 illustrates a representative wave speed at 100 Hz for a healthy control and a patient at the same location. The representative surface wave speeds were 3.69 and 1.97 m/s for the patient and healthy control, respectively. Three measurements were made for each frequency and at each location. Table 1 summarizes representative measurements of surface wave speed for a healthy control and a patient. Surface wave speed is expressed as the means ± standard deviation (SD) of the three measurements at each location and each frequency. The forearm

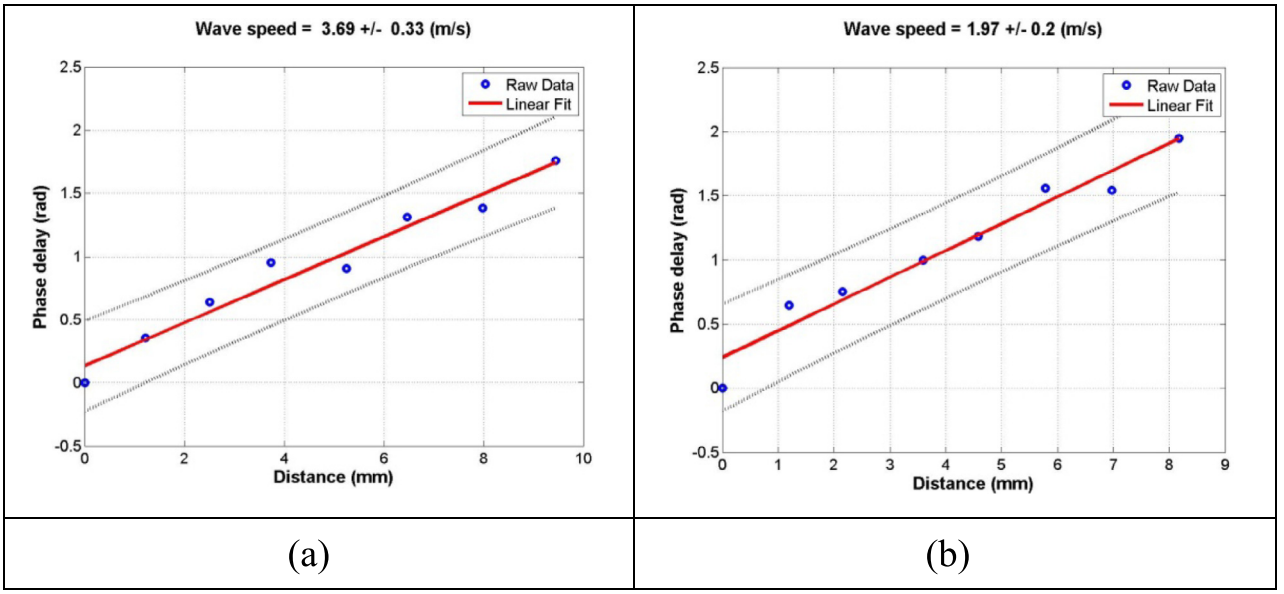

Fig. 4. The wave phase delay of the remaining locations, relative to the first location, is used to measure the surface wave speed. The slope of phase delay with distance measures the wave speed using eqn (7). Representative examples of wave speed at 100 Hz for a patient (a) and a healthy control (b).

and upper arm are designated by numbers 4 and 5, respectively. The right and left arms are designated by letters R and L, respectively. Therefore, R4 represents the skin of the right forearm.

Wave speeds of the 30 healthy controls and 41 patients at 100, 150 and 200 Hz are compared in Figure 5. The p values for the t-tests of the differences between patients and controls were less than 0.0001 for all four locations and three frequencies.

The elasticity and viscosity of skin tissue of the 30 healthy controls and 41 patients are compared in Figure 6. Viscoelasticity is estimated using eqn (6) with wave speed measurements at 100, 150 and 200 Hz. Most soft tissues have a mass density close to 1.0 g/cm^3. In the work described here, the mass density of skin was assumed to be 1.0 g/cm^3. The p values for the t-tests of the differences between patients and controls were less than 0.0001 for the four locations. Therefore, the magnitudes of both elasticity and viscosity were statistically higher for the patients than for the healthy controls.

Table 1. Representative surface wave speeds of a healthy control and a patient at four skin locations at 100, 150 and 200 Hz

	Surface wave speed (m/s)			
	R4	R5	L4	L5
Healthy control				
100 Hz	1.97 ± 0.31	1.7 ± 0.28	1.83 ± 0.04	1.79 ± 0.07
150 Hz	2.31 ± 0.08	2.5 ± 0.13	2.33 ± 0.25	2.52 ± 0.41
200 Hz	2.82 ± 0.19	2.99 ± 0.18	3.04 ± 0.37	3 ± 0.19
Patient				
100 Hz	3.42 ± 0.27	2.22 ± 0.25	2.82 ± 0.31	2.47 ± 0.22
150 Hz	4.52 ± 0.59	2.52 ± 0.35	3.6 ± 0.38	3.67 ± 0.25
200 Hz	5.17 ± 0.57	3.04 ± 0.23	5.36 ± 0.55	5.78 ± 0.64

In Figure 7 are representative ultrasound images of superficial lung tissue for a patient and a healthy control. The lung surface of healthy controls typically smooth, whereas the lung surface of patients is relatively rough. Table 2 summarizes the representative measurements of surface wave speed of lung for a healthy control and a patient. The three intercostal spaces are designated by numbers 1 to 3. The upper anterior lung is designated 1. The lower lungs at the lateral and posterior positions are designated 2 and 3, respectively. The right and left sides of the lung are designated by the letters "R" and "L", respectively. Therefore, L1 represents the left anterior lung in the second intercostal space.

Lung surface wave speeds of the 30 healthy controls and 41 patients at 100, 150 and 200 Hz are compared in Figure 8. The p values for the t-tests of the differences between patients and controls were less than 0.0001 for all intercostal spaces and for three frequencies.

DISCUSSION

The aim of this study was to translate an USWE technique into clinical use for quantitative assessment of patients with SSc and ILD. A high pulse repetition rate of 2000 frame/s was used to detect tissue motion in response to excitations of 100, 150 and 200 Hz. A Verasonics ultrasound system was used to collect up to a few thousand imaging frames per second using a plane-wave pulse trans-

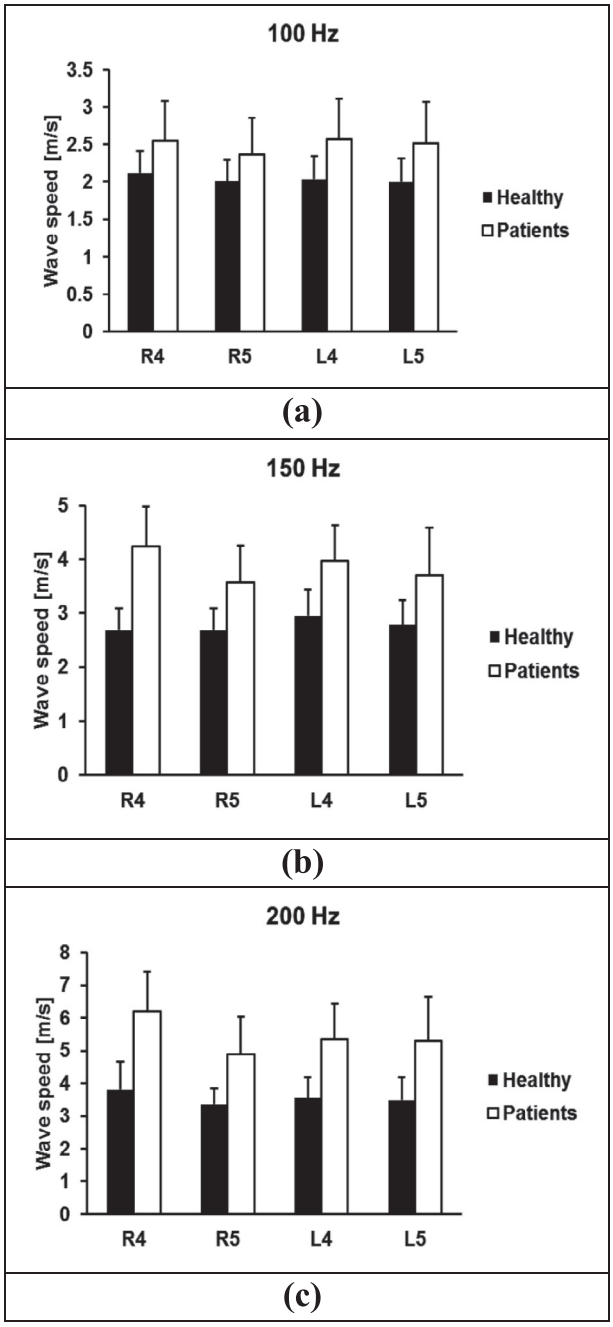

Fig. 5. Comparison of wave speeds between healthy controls and patients at four locations. Surface wave speeds at (a) 100 Hz, (b) 150 Hz and (c) 200 Hz. The *p* values for differences between the patients and controls were less than 0.0001 for all four locations and three frequencies, respectively.

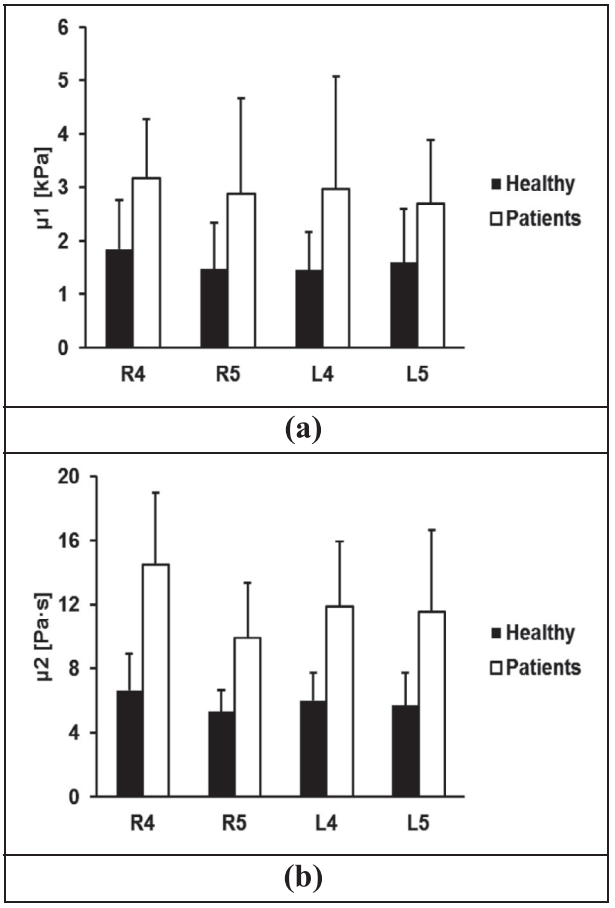

Fig. 6. Comparison of elasticity μ_1 (a) and viscosity μ_2 (b) between healthy controls and patients at four locations. The *p* values of differences between the patients and controls were less than 0.0001 for the four locations.

mission method. The skin motion velocities at these locations were measured in the normal direction of skin using the ultrasound tracking beams through those locations (Hasegawa and Kanai 2006; Zhang et al. 2011a, 2011b). The wave speed on the skin was measured by analyzing ultrasound data directly from the skin. Therefore, the wave speed measurement was local and independent of the location and amplitude of excitation. Surface wave speeds of skin of both left and right forearms and upper arms of both healthy controls and SSc patients were tested at three excitation frequencies, and their viscoelasticity was evaluated. The surface wave speeds of lung at six intercostal locations were measured at three excitation frequencies in healthy controls and SSc patients.

The results obtained in this study are in agreement with published results in literature. We found that the viscoelasticity of SSc patients is statistically higher than that of healthy controls. Skin of the peri-oral region of SSc patients was stiffer than that of healthy controls (Cannaò et al. 2014). Our earlier pilot work using an optical-based technique indicated that skin viscoelasticity was a more sensitive measure than palpation for assessing SSc (Zhang et al. 2011a, 2011b). Our technology was favorably reviewed by Yale dermatologists (Lott and Girardi 2011), who commented that this novel technology could benefit patients through new multimodal paradigms for assessing SSc.

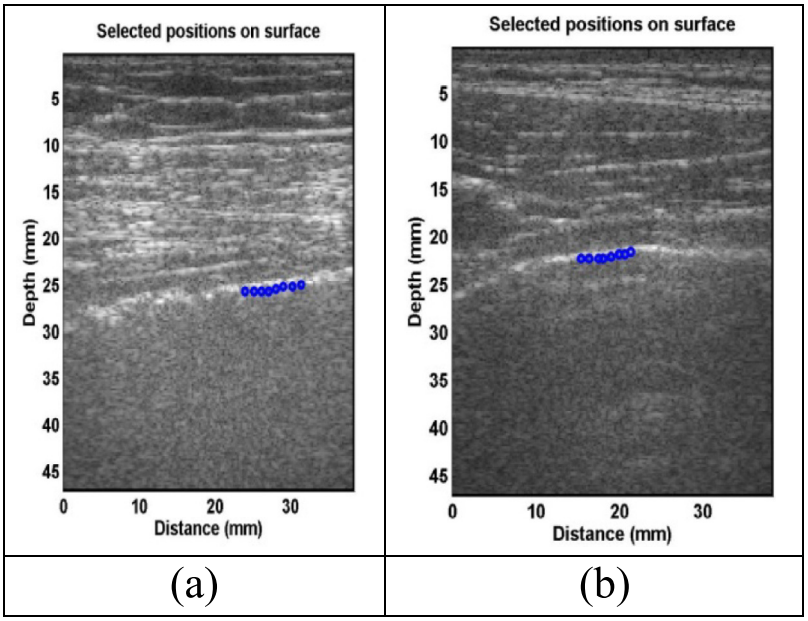

Fig. 7. Representative B-mode images of a lung for a patient (a) and a healthy control (b). The lung surfaces of healthy controls are typically smooth, whereas lung surfaces of patients are relatively rough.

Ultrasound elastography has been used to compare skin elasticity between SSc patients and healthy controls (Iagnocco et al. 2010). However, it provides only semiquantitative scales to characterize the elasticity of skin. and it is difficult to differentiate patients from healthy controls. USWE quantifies the viscoelasticity of skin tissue for SSc patients and provides accurate biomarkers for evaluating disease progression.

Optical coherence tomography (OCT) (Abignano et al. 2013; Shazly et al. 2015) and OCT-based elastography techniques (Li et al. 2014; Nguyen et al. 2014) provide high-spatial resolution of skin, but cannot measure deep subcutaneous tissue. The imaging penetration of OCT in skin can be up to 1.5 mm (Liang and Boppart 2010). Fibrosis affects not only skin, but also subcutaneous tissue (Li et al. 2007). One advantage of USWE is its capability to measure subcutaneous tissue (Kubo et al. 2017). In the current setup, subcutaneous tissues can be measured up to 45 mm (Figs. 2 and 6). USWE may be used to assess skin, subcutaneous connective tissue and muscle for patients with SSc.

Most ultrasound-based elastography techniques use ultrasound radiation force (URF) to generate tissue motion. Acoustic radiation force impulse imaging (ARFI) has recently been used to assess skin fibrosis (Hou et al. 2015; Lee et al. 2015). To generate sufficient tissue motion using URF, relatively high-intensity ultrasound energy is needed. Although URF has been used in most organs including the liver, URF should not be applied to the lung. *In vivo* animal lung studies have found that the relatively high-intensity ultrasound energy may cause alveolar hemorrhage or lung injury (Zachary et al. 2006). In addition, long periods of high-intensity ultrasound may damage the ultrasound system, for example, high voltage drop and probe element damage. In USWE, the surface wave on the lung is safely generated by a local mechanical vibration on the chest.

Table 2. Representative surface wave speeds of a healthy control and a patient through six intercostal spaces at 100, 150 and 200 Hz

	Surface wave speed (m/s)					
	R1	R2	R3	L1	L2	L3
Healthy control						
100 Hz	1.98 ± 0.07	1.83 ± 0.26	2.01 ± 0.23	2.07 ± 0.39	2.09 ± 0.3	1.95 ± 0.32
150 Hz	2.63 ± 0.46	2.65 ± 0.15	2.56 ± 0.16	2.61 ± 0.16	2.68 ± 0.12	2.52 ± 0.42
200 Hz	3.18 ± 0.58	3.28 ± 0.25	3.14 ± 0.13	2.98 ± 0.36	3.03 ± 0.2	3.1 ± 0.45
Patient						
100	3.26 ± 0.41	2.78 ± 0.34	3.25 ± 0.15	2.8 ± 0.39	2.79 ± 0.95	2.97 ± 0.26
150	3.86 ± 0.43	3.59 ± 0.41	4.36 ± 0.43	3.35 ± 0.61	3.13 ± 0.85	3.57 ± 0.02
200	4.19 ± 1.61	4.57 ± 0.13	5.79 ± 0.64	5.51 ± 0.51	4.63 ± 1.27	4.35 ± 1.03

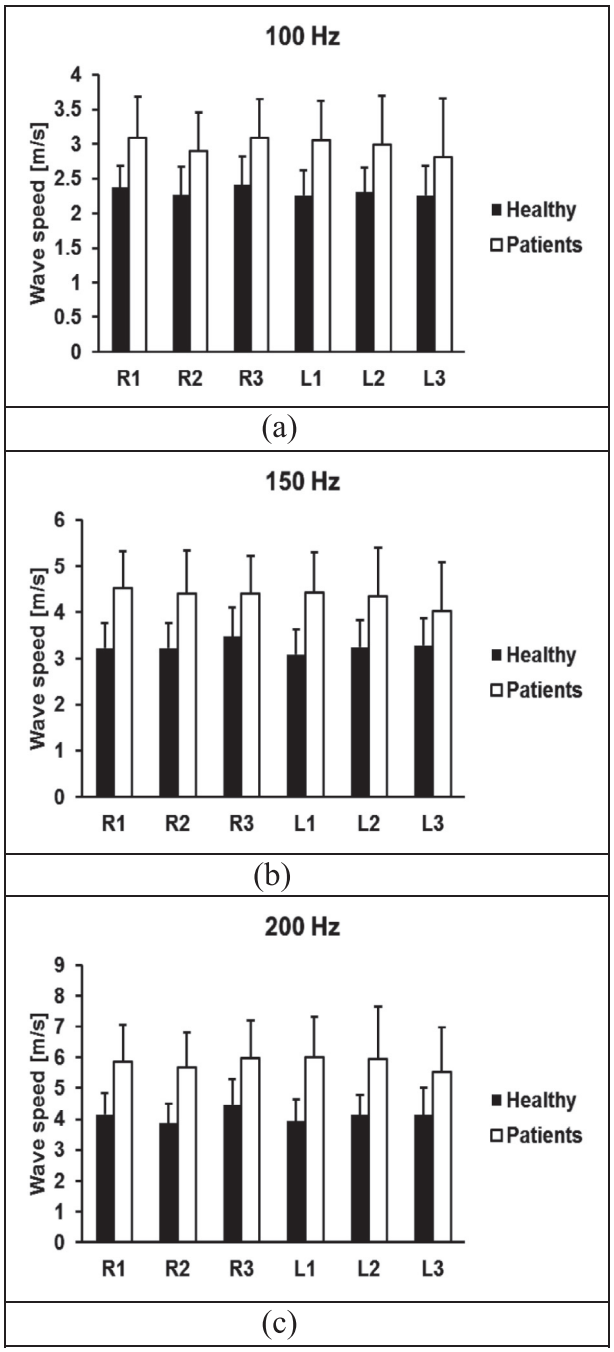

Fig. 8. Comparison of wave speeds between healthy controls and patients through six intercostal spaces. Surface wave speeds were measured at (a) 100 Hz, (b) 150 Hz and (c) 200 Hz. The p values for the differences between the patients and controls were less than 0.0001 for all intercostal spaces and for three frequencies.

Diagnostic ultrasound is used only for detecting surface wave propagation on the lung. Therefore, the USWE technique is a safe method for lung testing and patient screening. Moreover, because URF cannot be directly generated on surface tissue, a standoff pad is needed for exciting the skin. However, the standoff pad decays the URF and complicates the URF on the skin. In USWE, the mechanical excitation is directly applied to the skin and the standoff pad is used only to improve imaging of the skin. USWE provides a safe and simple way to generate and detect wave propagation on the skin. One advantage of USWE compared with most ultrasound elastography techniques is that the wave propagation is generated by a 0.1-s harmonic excitation rather than a short pulse using URF. The wave speed is measured quickly and accurately at a frequency with high signal-to-noise ratio. The tissue motion can be safely generated at a level of 20 μm using USWE. The radiation force ultrasound generated tissue motion is typically about 1~2 μm.

In USWE, the standoff pad is used only to improve imaging of the skin. We do not use the probe to generate pressure on the skin as in tissue stain imaging. In our testing, the gel pad sits on the skin surface naturally. The ultrasound probe is attached to the gel pad using ultrasound gel. We keep this experimental setup for each patient. We do not study the pressure effect on the skin measurements. However, we may investigate it by carefully controlling the generated pressure on the skin and measuring the associated surface wave speed changes. This may be useful to study non-linear or hyperelastic properties of the skin.

Heartbeat or tissue movement should not affect our skin and lung testing. The lung is tested at total lung volume when the participant takes a deep breath and holds it for a few seconds. The Arm skin is tested at normal breathing, and the arm rests on a pillow. We measure the surface wave speed at a given excitation frequency between 100 and 200 Hz, which is typically higher than the frequency of a heartbeat or tissue movement. We use triggering for acquisition. The trigger is used to synchronize the ultrasound wave measurement with the external vibration excitation.

In this study, we measured both skin and lung surface wave speeds of patients with SSc and ILD. High-resolution computed tomography (HRCT) is the clinical standard for diagnosing and characterizing lung fibrosis (Mathieson et al. 1989; Verschakelen 2010). However, HRCT exposes patients to ionizing X-ray radiation. USWE provides a non-invasive, safe method for measuring superficial lung tissues for assessing lung fibrosis (Kalra et al. 2017; Zhang et al. 2017). USWE may be useful as a screening tool in assessment of patients with ILD and complements HRCT as a follow-up tool for assessing progression of the disease.

We cannot find data on the mass density of the lungs of ILD patients. Lung density is also dependent on pulmonary pressure. In this research, participants were tested at total lung capacity (TLC) when taking a deep breath and holding it. In a study using an X-ray technique (Garnett et al. 1977), lung density was averaged to be 0.32 g/cm^3

for healthy lungs. The measurements were made with the patient sitting either on a chair or in bed and breathing quietly. Lung density was 0.33–0.93 g/cm^3 for patients with pulmonary congestion and edema. An *ex vivo* study of sheep lungs (Jahed et al. 1989) used a lung density of 0.19–0.26 g/cm^3. We expect that the lung density of ILD-affected lungs would be higher than that of healthy lungs. However, we were not able to find data on the lung density of ILD patients. We did not calculate lung viscoelasticity from the surface wave speeds measured in the work described here. The Surface wave speed alone provides good separation between the healthy controls and the patients with ILD in this research. We are very interested in studying the lung density of patients with ILD and the variation in lung density with pulmonary pressure.

Ultrasound surface wave elastography provides a novel, tolerable, non-invasive and non-ionizing technique for measuring skin and lung stiffness that may be useful for quantitative and effective assessment of both skin and lung diseases. We will further test the clinical utility of USWE in multiple fibrotic disorders. Many systemic diseases, including SSc (Steen and Medsger 2000), graft-versus-host disease (Hausermann et al. 2008), peripheral vascular disease (Spentzouris and Labropoulos 2009) and diabetic sclerosis (Van Hattem et al. 2008), are associated with skin stiffening from fibrosis.

CONCLUSION

Ultrasound surface wave elastography provides a non-invasive and non-ionizing technique to measure the surface wave speeds of both skin and superficial lung tissue. In this study, USWE was used to measure both skin and lung surface wave speeds for 41 patients with both SSc and ILD and 30 healthy controls. The surface wave speeds were measured at four locations on the arms at three excitation frequencies of 100, 150 and 200 Hz. Viscoelasticity of the skin was calculated from the wave speed dispersion with frequency using the Voigt model. The magnitudes of surface wave speed and viscoelasticity of diseased skin were significantly higher than those of healthy skin ($p < 0.0001$). The upper and lower lungs were measured through six intercostal spaces for patients and healthy controls. The magnitudes of surface wave speed of diseased lungs were significantly higher than those of healthy lungs ($p < 0.0001$) for each location and each frequency. USWE may be useful for quantitative assessment of SSc and/or ILD. We will investigate a larger population of ILD patients to study the relationship between skin stiffness and lung stiffness for patients with and without SSc.

Acknowledgments—This study is supported by National Institutes of Health Grant R01 HL125234 from the National Heart, Lung, and Blood Institute. We thank the anonymous reviewers for their encouraging and constructive comments. We thank Mrs. Jennifer Poston for editing this article. Without their assistance, this article would not have been presented in the current form.

REFERENCES

Abignano G, Aydin SZ, Castillo-Gallego C, Liakouli V, Woods D, Meekings A, Wakefield RJ, McGonagle DG, Emery P, Del Galdo F. Virtual skin biopsy by optical coherence tomography: The first quantitative imaging biomarker for scleroderma. Ann Rheum Dis 2013; 72:1845–1851.

Abignano G, Buch M, Emery P, Del Galdo F. Biomarkers in the management of scleroderma: An update. Curr Rheumatol Rep 2011;13: 4–12.

American Rheumatism Association Diagnostic and Therapeutic Criteria Committee, Subcommittee for Scleroderma Criteria. Preliminary criteria for the classification of systemic sclerosis (scleroderma). Arthritis Rheum 1980;23:581–590.

Boyer G, Laquieze L, Le Bot A, Laquieze S, Zahouani H. Dynamic indentation on human skin in vivo: Ageing effects. Skin Res Technol 2009;15:55–67.

Cannaò PM, Vinci V, Caviggioli F, Klinger M, Orlandi D, Sardanelli F, Serafini G, Sconfienza LM. Technical feasibility of real-time elastography to assess the peri-oral region in patients affected by systemic sclerosis. J Ultrasound 2014;17:265–269.

Catheline S, Gennisson JL, Delon G, Fink M, Sinkus R, Abouelkaram S, Culioli J. Measuring of viscoelastic properties of homogeneous soft solid using transient elastography: An inverse problem approach. J Acoust Soc Am 2004;116:3734–3741.

Chen S, Urban MW, Pislaru C, Kinnick R, Zheng Y, Yao A, Greenleaf JF. Shearwave dispersion ultrasound vibrometry (SDUV) for measuring tissue elasticity and viscosity. IEEE Trans Ultrason Ferroelectr Freq Control 2009;56:55–62.

Cicchetti DV. Guidelines, criteria, and rules of thumb for evaluating normed and standardized assessment instruments in psychology. Psychol Assess 1994;6:284–290.

Clements P, Lachenbruch P, Siebold J, White B, Weiner S, Martin R, Weinstein A, Weisman M, Mayes M, Collier D, Wigley F, Medsger T, Steen V, Moreland L, Dixon M, Massa M, Lally E, McCloskey D, Varga J. Inter and intraobserver variability of total skin thickness score (modified Rodnan TSS) in systemic sclerosis. J Rheumatol 1995;22:1281–1285.

Clements PJ, Hurwitz EL, Wong WK, Seibold JR, Mayes M, White B, Wigley F, Weisman M, Barr W, Moreland L, Medsger TA, Jr., Steen VD, Martin RW, Collier D, Weinstein A, Lally E, Varga J, Weiner SR, Andrews B, Abeles M, Furst DE. Skin thickness score as a predictor and correlate of outcome in systemic sclerosis: High-dose versus low-dose penicillamine trial. Arthritis Rheum 2000;43:2445–2454.

Clements PJ, Lachenbruch PA, Ng SC, Simmons M, Sterz M, Furst DE. Skin score: A semiquantitative measure of cutaneous involvement that improves prediction of prognosis in systemic sclerosis. Arthritis Rheum 1990;33:1256–1263.

Coultas DB, Zumwalt RE, Black WC, Sobonya RE. The epidemiology of interstitial lung diseases. Am J Respir Crit Care Med 1994;150: 967–972.

Delle Sedie A, Carli L, Cioffi E, Bombardieri S, Riente L. The promising role of lung ultrasound in systemic sclerosis. Clin Rheumatol 2012;31:1537–1541.

Desai SR, Veeraraghavan S, Hansell DM, Nikolakopolou A, Goh NS, Nicholson AG, Colby TV, Denton CP, Black CM, du Bois RM, Wells AU. CT features of lung disease in patients with systemic sclerosis: Comparison with idiopathic pulmonary fibrosis and nonspecific interstitial pneumonia. Radiology 2004;232:560–567.

Garnett ES, Webber CE, Coates G, Cockshott WP, Nahmias C, Lassen N. Lung density: Clinical method for quantitation of pulmonary congestion and edema. Can Med Assoc J 1977;116:153–154.

Hasegawa H, Kanai H. Improving accuracy in estimation of artery-wall displacement by referring to center frequency of RF echo. IEEE Trans Ultrason Ferroelectr Freq Control 2006;53:52–63.

Hausermann P, Walter RB, Halter J, Biedermann BC, Tichelli A, Itin P, Gratwohl A. Cutaneous graft-versus-host disease: A guide for the dermatologist. Dermatology 2008;216:287–304.

Hendriks FM, Brokken D, Oomens CW, Bader DL, Baaijens FP. The relative contributions of different skin layers to the mechanical behavior of human skin in vivo using suction experiments. Med Eng Phys 2006;28:259–266.

Hou Y, Zhu QL, Liu H, Jiang YX, Wang L, Xu D, Li MT, Zeng XF, Zhang FC. A preliminary study of acoustic radiation force impulse quantification for the assessment of skin in diffuse cutaneous systemic sclerosis. J Rheumatol 2015;42:449–455.

Iagnocco A, Kaloudi O, Perella C, Bandinelli F, Riccieri V, Vasile M, Porta F, Valesini G, Matucci-Cerinic M. Ultrasound elastography assessment of skin involvement in systemic sclerosis: Lights and shadows. J Rheumatol 2010;37:1688–1691.

Jahed M, Lai-Fook SJ, Bhagat PK, Kraman SS. Propagation of stress waves in inflated sheep lungs. J Appl Physiol 1989;66:2675–2680.

Kalra S, Osborn T, Bartholmai B, Zhou B, Zhang X. 2017 Lung ultrasound surface wave elastography-preliminary measurements in patients with interstitial lung diseases. Respirology 2017;22(S2):18–100.

Kissin EY, Schiller AM, Gelbard RB, Anderson JJ, Falanga V, Simms RW, Korn JH, Merkel PA. Durometry for the assessment of skin disease in systemic sclerosis. Arthritis Rheum 2006;55:603–609.

Kubo K, Zhou B, Cheng YS, Yang TH, Qiang B, An KN, Moran SL, Amadio PC, Zhang X, Zhao C. Ultrasound elastography for carpal tunnel pressure measurement: A cadaveric validation study. J Orthop Res 2017;doi:10.1002/jor.23658. [Epub ahead of print].

Lee SY, Cardones AR, Doherty J, Nightingale K, Palmeri M. Preliminary results on the feasibility of using ARFI/SWEI to assess cutaneous sclerotic diseases. Ultrasound Med Biol 2015;41:2806–2819.

Li C, Guan G, Zhang F, Nabi G, Wang RK, Huang Z. Laser induced surface acoustic wave combined with phase sensitive optical coherence tomography for superficial tissue characterization: A solution for practical application. Biomed Opt Express 2014;5:1403–1419.

Liang X, Boppart SA. Biomechanical properties of in vivo human skin from dynamic optical coherence elastography. IEEE Trans Biomed Eng 2010;7:953–959.

Lott JP, Girardi M. Practice gaps: The hard task of measuring cutaneous fibrosis. Arch Dermatol 2011;147:1115–1116.

Mathieson JR, Mayo JR, Staples CA, Muller NL. Chronic diffuse infiltrative lung disease: Comparison of diagnostic accuracy of CT and chest radiography. Radiology 1989;171:111–116.

Mayo JR. CT evaluation of diffuse infiltrative lung disease: Dose considerations and optimal technique. J Thorac Imaging 2009;24:252–259.

Merkel PA, Silliman NP, Denton CP, Furst DE, Khanna D, Emery P, Hsu VM, Streisand JB, Polisson RP, Akesson A, Coppock J, van den Hoogen F, Herrick A, Mayes MD, Veale D, Seibold JR, Black CM, Korn JH. Validity, reliability, and feasibility of durometer measurements of scleroderma skin disease in a multicenter treatment trial. Arthritis Rheum 2008;59:699–705.

Miller GF, Pursey H. The field and radiation impedence of mechanical radiatiors on the free surface of a semi-infinite isotropic solids. Proc R Soc London A Math Phys Sci 1954;223:521–541.

Nguyen TM, Song S, Arnal B, Wong EY, Huang Z, Wang RK, O'Donnell M. Shear wave pulse compression for dynamic elastography using phase-sensitive optical coherence tomography. J Biomed Opt 2014;19:16013.

Nkemzi D. A new formula for the velocity of Rayleigh waves. Wave Motion 1997;26:199–205.

Pailler-Mattei C, Bec S, Zahouani H. In vivo measurements of the elastic mechanical properties of human skin by indentation tests. Med Eng Phys 2008;30:599–606.

Postlethwaite AE, Wong WK, Clements P, Chatterjee S, Fessler BJ, Kang AH, Korn J, Mayes M, Merkel PA, Molitor JA, Moreland L, Rothfield N, Simms RW, Smith EA, Spiera R, Steen V, Warrington K, White B, Wigley F, Furst DE. A multicenter, randomized, double-blind, placebo-controlled trial of oral type I collagen treatment in patients with diffuse cutaneous systemic sclerosis: I. Oral type I collagen does not improve skin in all patients, but may improve skin in late-phase disease. Arthritis Rheum 2008;58:1810–1822.

Prim DA, Zhou B, Hartstone-Rose A, Uline MJ, Shazly T, Eberth JF. A mechanical argument for the differential performance of coronary artery grafts. J Mech Behav Biomed Mater 2016;54:93–105.

Royer D, Clorennec D. An improved approximation for the Rayleigh wave equation. Ultrasonics 2007;46:23–24.

Serup J, Jemec GBE. Handbook of non-invasive methods and the skin. Boca Raton, FL: CRC Press; 1995.

Shazly T, Rachev A, Lessner S, Argraves WS, Ferdous J, Zhou B, Moreira AM, Sutton M. On the uniaxial ring test of tissue engineered constructs. Exp Mech 2015;55:41–51.

Smalls LK, Randall Wickett R, Visscher MO. Effect of dermal thickness, tissue composition, and body site on skin biomechanical properties. Skin Res Technol 2006;12:43–49.

Spentzouris G, Labropoulos N. The evaluation of lower-extremity ulcers. Semin Intervent Radiol 2009;26:286–295.

Steen VD, Medsger TA, Jr. Severe organ involvement in systemic sclerosis with diffuse scleroderma. Arthritis Rheum 2000;43:2437–2444.

Steen VD, Medsger TA, Jr. Improvement in skin thickening in systemic sclerosis associated with improved survival. Arthritis Rheum 2001;44:2828–2835.

Twal WO, Klatt SC, Harikrishnan K, Gerges E, Cooley MA, Trusk TC, Zhou B, Gabr MG, Shazly T, Lessner SM. Cellularized microcarriers as adhesive building blocks for fabrication of tubular tissue constructs. Ann Biomed Eng 2014;42:1470–1481.

Van Hattem S, Bootsma AH, Thio HB. Skin manifestations of diabetes. Cleve Clin J Med 2008;75:passim.

Verschakelen JA. The role of high-resolution computed tomography in the work-up of interstitial lung disease. Curr Opin Pulm Med 2010;16:503–510.

Viktorov I. Raleigh and Lamb waves. New York: Plenum Press; 1976.

Vinh PC, Malischewsky PG. An improved approximation of Bergmann's form for the Rayleigh wave velocity. Ultrasonics 2007;47:49–54.

Wells AU, Hansell DM, Rubens MB, Cullinan P, Black CM, du Bois RM. The predictive value of appearances on thin-section computed tomography in fibrosing alveolitis. Am Rev Respir Dis 1993;148:1076–1082.

Zachary JF, Blue JP, Jr., Miller RJ, Ricconi BJ, Eden JG, O'Brien WD, Jr. Lesions of ultrasound-induced lung hemorrhage are not consistent with thermal injury. Ultrasound Med Biol 2006;32:1763–1770.

Zhang X, Greenleaf JF. Estimation of tissue's elasticity with surface wave speed. J Acoust Soc Am 2007;122:2522–2525.

Zhang X, Osborn T, Kalra S. A noninvasive ultrasound elastography technique for measuring surface waves on the lung. Ultrasonics 2016;71:183–188.

Zhang X, Osborn T, Zhou B, Bartholmai B, Greenleaf JF, Kalra S. An ultrasound surface wave elastography technique for noninvasive measurement of surface lung tissue. J Acoust Soc Am 2017;141:3721.

Zhang X, Osborn TG, Pittelkow MR, Qiang B, Kinnick RR, Greenleaf JF. Quantitative assessment of scleroderma by surface wave technique. Med Eng Phys 2011a;33:31–37.

Zhang X, Qiang B, Hubmayr RD, Urban MW, Kinnick R, Greenleaf JF. Noninvasive ultrasound image guided surface wave method for measuring the wave speed and estimating the elasticity of lungs: A feasibility study. Ultrasonics 2011b;51:289–295.

Zhou B, Sit AJ, Zhang X. Noninvasive measurement of wave speed of porcine cornea in ex vivo porcine eyes for various intraocular pressures. Ultrasonics 2017;81:86–92.